GRAIN BOUNDARY GEOMETRY AND INTERGRANULAR CRACK PROPAGATION IN Ni_3Al AND Ir

Hui Lin and David P. Pope

Department of Materials Science and Engineering, University of Pennsylvania
3231 Walnut Street, Philadelphia, PA 19104, U.S.A.

Abstract

The distribution of grain boundary types along intergranular cracks in B-free Ni_3Al and pure Ir was measured, by Σ value, and compared to the distribution in the bulk, using statistically significant sample sizes. It was found that low angle ($\Sigma 1$) and symmetrical $\Sigma 3$ boundaries (twins) are particularly strong. All other high boundaries have similarly low strength, independent of their Σ values, in particular, low Σ, high angle boundaries, as a group, are not strong. These results qualitatively agree with predictions based on the structural unit model and imply that 1) Ni_3Al and Ir have similar boundary structure and 2) the fracture strength of an intergranularly brittle polycrystalline aggregate can be increased only by increasing the fraction of low angle and symmetrical $\Sigma 3$ boundaries.

The authors wish to thank Dr. John Liu of ALCOA Technical Center and Dr. John Hack of Yale University for providing access to their EBSP facilities. This work was supported by the NSF MRL program under grant number DMR-88-19885 through the Laboratory for Research on the Structure of Matter at the University of Pennsylvania.

Superalloys 1992
Edited by S.D. Antolovich, R.W. Stusrud, R.A. MacKay,
D.L. Anton, T. Khan, R.D. Kissinger, D.L. Klarstrom
The Minerals, Metals & Materials Society, 1992

Introduction

This paper deals with the relationship between the structure and intrinsic cracking resistance of grain boundaries in fcc materials and fcc-based ordered intermetallic compounds. The experimental program centers on one simple case, intergranular fracture at low temperatures caused by the intrinsic weakness of grain boundaries, thereby avoiding the complexities associated with diffusion and/or impurity induced intergranular cracking and making it possible to reveal the purely structural relations. If the variation in fracture strength among grain boundaries of different character is sufficiently large that a class of strong boundaries can be identified then materials prone to intergranular cracking may be toughened by increasing the abundance of those "strong boundaries", a process called "grain boundary engineering" [1, 2]. Based on the information currently available in the literature [3-8], low angle ($\Sigma 1$) and $\Sigma 3$ boundaries in both fcc and bcc materials and possibly $\Sigma 11b$ {113}/{113} and $\Sigma 17b$ {223}/{223} twin boundaries in bcc materials are the only experimentally observed strong boundaries. Other boundaries, including a number of other low Σ boundaries, show lower and approximately equal strengths. However the statistical significance of much of these data is open to question.

We have identified types of strong boundaries in a statistically significant manner by performing specially designed bending tests on B-free Ni_3Al ($L1_2$ intermetallic) and pure Ir (fcc element) polycrystalline specimens. B-free Ni_3Al and Ir were chosen as the model materials in our study because they fail in a brittle intergranular manner at room temperature, even when the boundaries are impurity-free [9-13]. We have used specimens that are one grain thick, thereby avoiding the complications in the stress state due to subsurface grains. The stress state in such a specimen under bending can be approximated by that in a rectangular beam and the only non-zero stress component is an axial tensile stress which is maximal at the surface. Our approach is to first fracture the sample, then replace the broken pieces in their original, correct relative orientations, and then measure the grain orientations across the broken boundaries. The distributions of boundary types along the crack is then compared with the distribution obtained from the bulk to see if there are differences. The boundaries missing from the crack faces are then the strong grain boundaries. We have chosen to use Σ values from the CSL model , for reviews see [14-17], to classify boundaries, as have most previous investigators [8, 18-21]. We are also able to determine the boundary plane for certain boundaries and have done so for one set of strong boundaries.

The objectives of this study are: (1) to firmly establish the phenomenological relationship between grain boundary structure and intergranular crack propagation, (2) to identify which are the "strong boundaries", and (3) to relate the experimental results to the theory of boundary structure. This study is made possible by three factors: the use of one-grain-thick specimens, the ability to replace the cracked faces in their original positions, and the use of a semi-automated electron backscattering pattern (EBSP) technique to quickly orient a large number of grains.

Experimental

Melt-spun Ni_3Al ribbons (75.0 at.% Ni, 24.8 at.% Al and 0.2 at.% Ta, about 15mmx3mmx20μm) were used as specimens. These ribbons were first annealed at 1200°C for one hour in a 10^{-6} torr vacuum to allow individual grains to grow through the thickness of the ribbons. Both surfaces of the annealed ribbons were then mechanically polished to remove the alumina/spinel scale. A second anneal was then necessary to obtain sharp EBSP images. Two different treatments were used: one, which reveals grain boundaries through thermal etching, is a one-hour anneal at 1200°C in a 10^{-6} torr vacuum with a graphite oxygen getter, and the other, which results in no etching, is the same treatment at a temperature of 800°C. The Ir specimens (15mmx10mmx40μm) were made from hot-rolled sheets (99.99%) which were subsequently treated similarly to the Ni_3Al ribbons except that the first anneal was at 1700°C for 24 hours and the second anneal was at 1200°C for one hour resulting in a slight thermal etching.

A piece of Ni_3Al or Iridium ribbon thus prepared is then bonded with M-Bond 200 adhesive to a piece of clean 100 μm-thick aluminum foil using the same procedure as for mounting strain gages [22]. The composite is bent in air around an edge having a 3 mm radius of curvature to produce cracks in the ribbon. The whole piece is then flattened between two steel blocks and mounted on an SEM sample mount using carbon paint as an adhesive. (There are more than 3000 grains within the total bent region and about 50 grains in a given cross section, all under more or less the same tensile stress during bending. This means that there is a large number of grain boundaries available for crack initiation during any given bending test, and therefore the crack path is selected by the fracture process itself rather than by a localized stress concentration.)

The crystallographic orientations of individual grains, from which misorientations of grain-pairs are calculated and Σ values are assigned [23], were measured using the electron backscattering pattern (EBSP) method [24]. For all cubic systems the CSL relations are identical [25], thus the CSL relations for an $L1_2$ lattice are calculated in the same way as for an fcc lattice. We use the Brandon criterion [26] as the upper limit for near-coincidence boundaries, assign the lowest Σ value to a boundary if it qualifies for more than one near-Σ boundary, and arbitrarily set the upper limit of low Σ boundaries as Σ=49.

Results

Due to the limitation of space, we will only show the results from thermally etched Ni_3Al specimens with small cracks, Fig. 1a, and slightly etched Ir specimens with long cracks, Fig. 1b. However, the distribution of types of cracked boundaries is unaffected by thermal-etching of the grain boundaries and by changing the length of cracks from a few grain boundaries to a few hundred grain boundaries long [27]. Fracture surfaces of Ni_3Al and Iridium ribbon are shown in

Figs. 2a and 2b, respectively. Specimens used in this study are slightly textured-Ni_3Al has a <111> and Ir has a <100> texture.

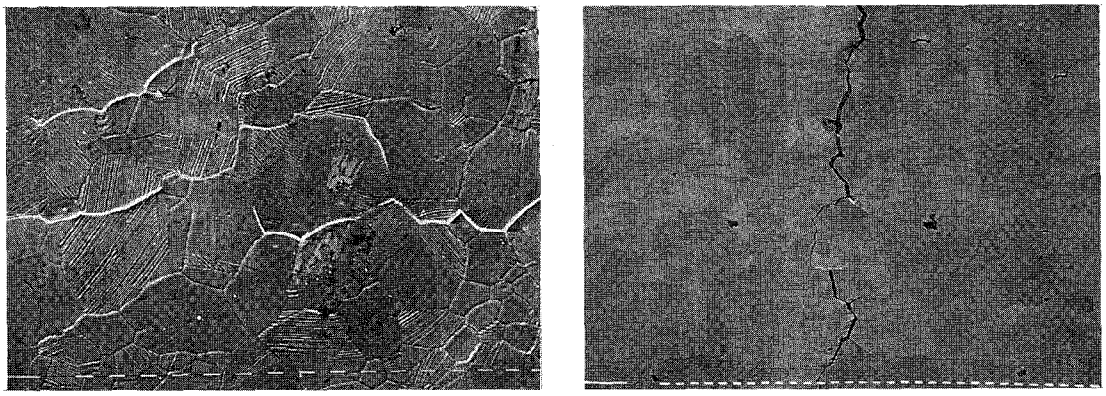

Fig. 1 Scanning electron micrographs (SEMs) showing the surface of (a), on the left, a thermally etched Ni_3Al specimen with small cracks (bright region) and (b), on the right, a slightly etched Ir specimens with long cracks (dark region). Each individual marker is 10 μm long.

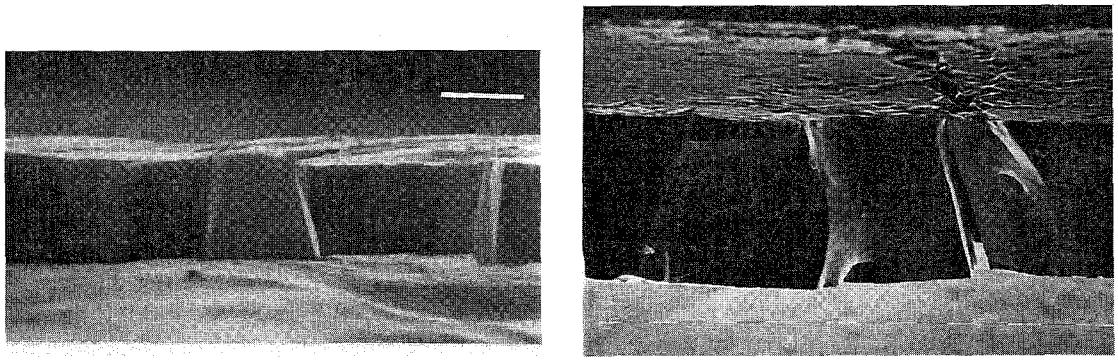

Fig. 2 SEMs of the intergranular surface of (a), on the left, an Ni_3Al and (b), on the right, an Ir specimen. Note that both specimens are one grain thick. Each marker is 10 μm long.

Thermally etched Ni_3Al specimen with small cracks

Table I lists in columns 2 and 3 the distribution of low angle, Σ3, low Σ and high Σ boundaries at random positions, by number and by percentage, respectively; in column 4, the 90% confidence intervals for 155 cracked boundaries, with the proportions in column 3 taken as the true proportions; in columns 5 and 6, the distribution of cracked low angle, Σ3, low Σ and high Σ boundaries in specimen 1, by number and by percentage, respectively; and in column 7, whether the percentages of cracked boundaries fall into their respective 90% confidence intervals*. The 90% confidence intervals are used as a check to see if the collected data scatter within some reasonable range of certain target values [28]. The data for $3<\Sigma\leq25$, a subset of the data for $3<\Sigma\leq49$, are included to check the possible effect of the arbitrary upper limit of low Σ boundaries. The same data are also plotted in Fig. 3a.

*The 90% confidence interval is the interval about the true mean of a distribution such that the probability is 0.9 that the mean of a sample of size N from that distribution will lie in that interval.

Table I The distribution of cracked boundaries compared with that in the general population in a thermally etched Ni_3Al specimen with small cracks.

Grain Boundary	General Population (A Total of 280 GB's)			Cracked (A Total of 155 GB's)		
Type by Σ value	No.	Percent	90% interval for 155 GB's	No.	Percent	Within Interval?
low angle	21	7.5%	4.5-11.0%	3	1.9%	no
Σ3	79	28.2%	22.6-33.5%	3	1.9%	no
($3 < \Sigma \leq 25$)	(12)	(4.3%)	(1.9-7.1%)	(8)	(5.8%)	yes
$3 < \Sigma \leq 49$	16	5.7%	3.2-8.4%	11	7.1%	yes
$\Sigma > 49$	164	58.6%	52.3-65.2%	138	89.0%	no
Total	280	100%		155	100%	

The total percentages of low Σ boundaries ($3 < \Sigma \leq 25$) in the general population is slightly different from that of an ideal untextured material, which is 7.47% [29]. For the two groups of low Σ boundaries, $3 < \Sigma \leq 25$ and $3 < \Sigma \leq 49$, the total percentages along cracks are close to that in the general population and lie within the 90% confidence limits. The similarity between the two sets of data indicates that the upper limit of low Σ boundaries is indeed arbitrary and insignificant. The percentages of low angle and Σ3 boundaries is much lower along cracks than those in the general population, indicating that these types of grain boundaries are resistant to intergranular cracking. The difference of about 20 percent in the proportion of high Σ boundaries can be attributed to the deficit of low angle and Σ3 boundaries along the crack.

As a check to see if the boundary distribution in the general population is representative of the distribution in the area near the cracks, table II compares the distribution of boundary types near the cracks (within 4-5 grains from the cracks) with that in the general population. The same data are also plotted in Fig. 3b. Note that the proportion of Σ3 boundaries at the two positions appears to be different. This suggests that the crack tends to select regions of the sample where there is a slightly lower fraction of Σ3 boundaries. The distribution of the remaining types of boundaries near cracks agrees well with that in the general population.

Table II The distribution of near-crack boundaries compared with that in the general population in a thermally etched Ni_3Al specimen with small cracks.

Grain Boundary	General Population (A Total of 280 GB's)			Near Crack (A Total of 259 GB's)		
Type by Σ value	No.	Percent	90% interval for 259 G.B.s	No.	Percent	Within Interval?
low angle	21	7.5%	5.0-10.0%	24	9.3%	yes
Σ3	79	28.2%	23.9-32.4%	56	21.6%	no
($3 < \Sigma \leq 25$)	(12)	(4.3%)	(2.3-6.2%)	(9)	(5.3%)	yes
$3 < \Sigma \leq 49$	16	5.7%	3.5-8.1%	17	6.6%	yes
$\Sigma > 49$	164	58.6%	53.7-63.3%	162	62.5%	yes
Total	280	100%		259	100%	

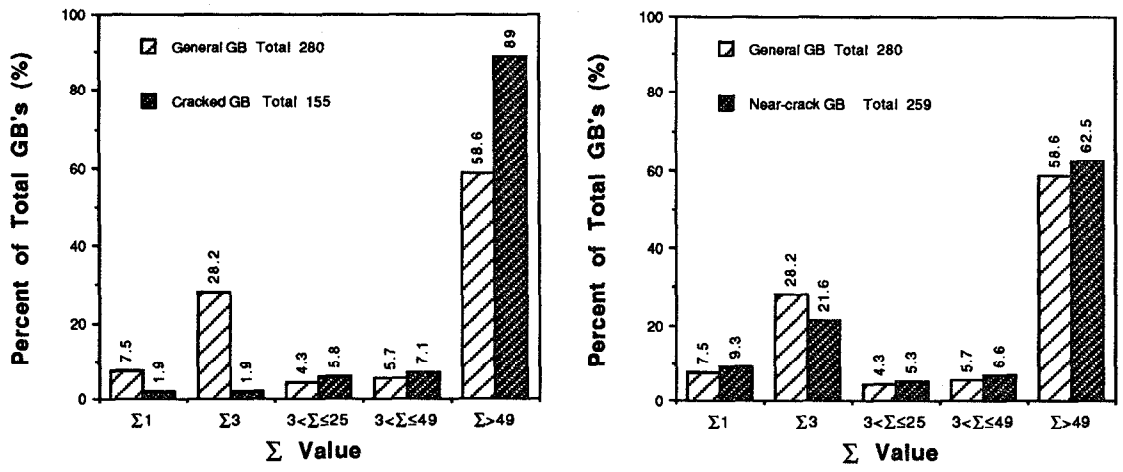

Fig. 3 The distribution of grain boundary types by Σ values for (a), on the left, cracked and (b), on the right, near-crack grain boundaries compared to that in the general population in an Ni_3Al specimen. The data are taken from table I and II, respectively.

Since Σ3 grain boundaries are found to resist intergranular cracking we set out to measure the grain boundary planes of these boundaries using the stereographic projection method [23]. We have arbitrarily defined a Σ3 boundary as being a near-symmetrical twin if the boundary plane deviates by no more than 5° from the {111} or {112} plane. For simplicity, we will call a near-symmetrical Σ3 boundary as a symmetrical Σ3 boundary, analogous to a near-coincidence boundary. A total of 20 Σ3 grain boundaries were randomly chosen out of the previously-indexed Σ3 boundaries in the specimen and the boundary planes were determined. The majority of the Σ3 grain boundaries are symmetrical twins with either {111}/{111} or {112}/{112} planes, see Table III. The three Σ3 boundaries in the specimen which broke during bending were all found to be non-symmetrical Σ3 boundaries.

Table III The distribution of types of Σ3 boundaries in a Ni_3Al specimen.

Types of Σ3 Boundary	Number	Percent
non-symmetrical	2	10%
symmetrical {112}/{112}	5	25%
symmetrical {111}/{111}	13	65%
Total	20	100%

Slightly etched Ir specimen with long cracks

The distribution of cracked boundaries along long cracks is listed in table III and compared with that of the general population. The same data are also plotted in Fig. 4. Note the similarity in the results for Ni_3Al and Ir (compare Figs. 3a and 4).

Table IV The distribution of cracked boundaries compared with that in the general population in a slightly etched Iridium specimen with long cracks.

Grain Boundary	General Population (A Total of 206 GB's)			Cracked (A Total of 83 GB's)		
Type by Σ value	No.	Percent	90% interval for 83 GB's	No.	Percent	Within Interval?
low angle	17	8.2%	3.6-12.0%	0	0.0%	no
Σ3	48	23.3%	20.5-36.1%	2	2.4%	no
(3 < Σ ≤ 25)	(11)	(5.3%)	(1.1-7.2%)	(6)	(7.2%)	yes
3 < Σ ≤ 49	15	7.3%	2.4-9.6%	7	8.4%	yes
Σ > 49	126	61.2%	50.6-67.5%	74	89.2%	no
Total	206	100%		83	100%	

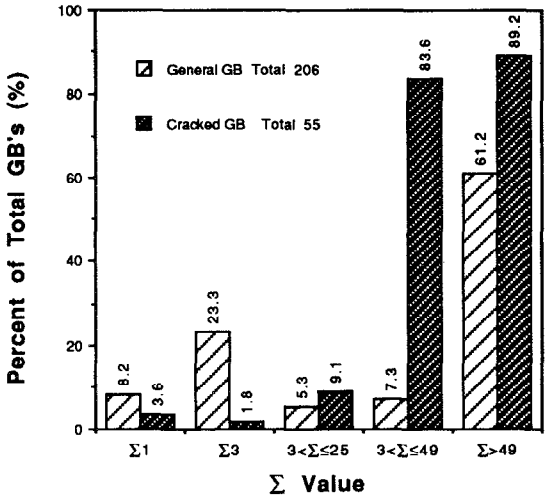

Fig. 4 The distributions of grain boundary types by Σ values for cracked grain boundaries compared to that in the general population in an Ir specimen with long cracks. The data are taken from table IV.

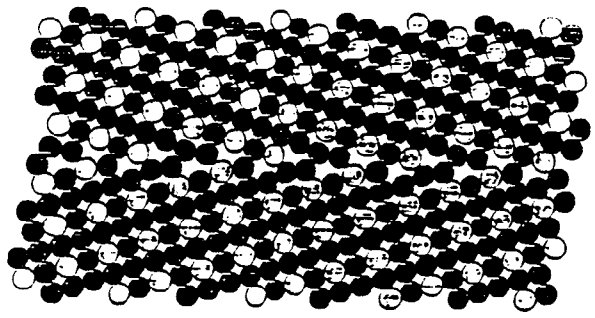

Fig. 5 A relaxed Σ5 (310) symmetrical tilt boundary in Ni_3Al [39]. The darker circles are Ni atoms and lighter ones are Al atoms. Note the cavities in the boundary.

Discussion

Implication of the results, nucleation vs. propagation

The distribution of boundary types along a crack depends on both the crack propagation path and the crack initiation sites if a given crack contains more than one initiation site. However the small, unconnected cracks (about 10 grain boundaries long) probably have only one initiation site for each crack and therefore the initiation sites constitute about 10% of the total for the short cracks and a smaller fraction for the longer cracks. Furthermore, since the fracture surfaces were not exposed, these nucleation sites cannot be easily identified. This means that correlations between boundary geometry and crack path made in this study relate mainly to crack propagation and contain little information about nucleation. Consequently, we conclude that Σ value has little effect on crack propagation in Ni_3Al and Ir since low Σ and high Σ boundaries fail with equal probability, except for Σ1 and symmetrical Σ3 (twins). These two kinds of boundaries resist

crack propagation and therefore are strong. Other boundaries have similarly low strengths, in particular,.low Σ boundaries, as a group, are not strong.

Comparison with theoretical models

The fact that low angle and symmetrical $\Sigma 3$ boundaries are strong and other boundaries have similarly low strengths, independent of Σ, is in accord with the implications of the structural unit model [30-34]. According to this model, for pure tilt boundaries, certain favored boundaries with only one type of units are the fundamental structural units of longer-period, or non-favored, tilt boundaries. A non-favored boundary in the misorientation range between those of the two successive favored boundaries is composed of well-defined mixtures of two different units of the two favored boundaries. The closer the misorientation is to one favored boundary, the more units of that favored boundary the non-favored boundary contains, and the boundary structure changes continuously throughout the misorientation range. Favored boundaries are generally low Σ boundaries [32], **but** not all low Σ boundaries are favored boundaries. Since the structure of a boundary having a misorientation angle between those of two favored boundaries is just a combination of the structural units of those two boundaries, the properties of the boundary are expected to vary continuously between those of the two favored boundaries. That is, a high Σ boundary can have properties, such as cohesion and the ability to produce local shear, similar to that of a low Σ boundary since favored boundaries are, generally, low Σ boundaries. In particular, when one of the favored boundaries is the ideal lattice, or has a structure similar to that of the ideal lattice, then boundaries containing units of this particular favored boundary should have properties similar to that of the ideal lattice.

Crack propagation is believed to be the results of low cohesion and difficulty in producing local shear [35], and we think this is equally true for Ni_3Al (ordered fcc) and Ir (fcc). However, we will focus on Ni_3Al in the following discussion (much is understood about the structure of grain boundaries in Ni_3Al but little about that in Ir) then draw some parallels between Ir and Ni_3Al. Ni_3Al is ductile in single crystalline form-the ideal lattice has high cohesion and can easily plastically deform, both locally and globally. Therefore any boundary containing large portions of the ideal lattice should also possess these qualities. Low angle boundaries are essentially ideal lattice containing periodically-spaced dislocation cores [36]. The interfacial region in a $\Sigma 3$ $\{111\}/\{111\}$ boundary has a structure identical to that of the ideal lattice and a $\Sigma 3$ $\{112\}/\{112\}$ boundary has an interface slightly distorted from that of the ideal lattice, based on simulations of grain boundary structure using empirically-constructed interatomic potentials [37]. Thus low angle and symmetrical $\Sigma 3$ boundaries should be able to resist crack propagation and therefore be strong, and our results confirm this prediction. Most other boundaries cannot resist crack propagation because they are structurally different from the ideal lattice and contain defects. Takasugi and Izumi first postulated that strongly ordered intermetallics have cavities in certain low Σ boundaries based on geometrical considerations and the assumption that strict chemical

bonding is maintained up to the boundaries [38]. Later, Vitek et al found large cylindrical cavities of atomic size in strongly ordered intermetallics similar to Ni_3Al, see Fig. 5, based on atomistic studies of a number of favored symmetrical tilt boundaries [39]. There are varying degrees of distortion in different favored boundaries and the same distortions are inherited in the non-favored boundaries. As a result, the boundaries which contain cavities is expected to have much lower local cohesive strengths than that of those without cavities (due, perhaps, to the heterogeneity of the electron density in the boundaries [40]) and difficulty of producing local shear (due to the irregular arrangement of atoms near the boundaries). Therefore high angle boundaries, independent of their Σ values, are expected to be less resistant to crack propagation and our results confirm this prediction.

We suspect that the above reasoning would be applicable to Ir even though little is known about the structure of grain boundaries in that material. The similarity in intergranular cracking-resistance between Ni_3Al and Ir may be a result of a similarity in the grain boundary structure. High angle boundaries in Ir may also have cavities because Ir has some fundamental properties similar to those of Ni_3Al. For example, the Cauchy pressure, C_{12}-C_{44}, for Ir is negative while it is positive for most ductile fcc materials [39]. Similarly, the Cauchy pressure for Ni_3Al and other early transition metal trialuminides is negative while it is positive for most other aluminides [40]. A negative Cauchy pressure indicates that the angular character to the atomic bonding is important. In other words, materials with negative values of Cauchy pressure have highly directional bonding, instead of homogeneous metallic bonding. The directional bonding increases the bond energy resulting in a high melting temperature for Ir (2410°C) and a high ordering energy for Ni_3Al. It also necessitates the formation of grain boundary cavities in high angle boundaries because the directionality of the bonding across such a boundary can only be maintained by decreasing the local packing efficiency. Therefore Ir would have an intergranular cracking-resistance similar to that of Ni_3Al, as indicated by our results.

Conclusions

In B-free Ni_3Al and pure Ir:

1. Low angle ($\Sigma 1$) boundaries and symmetrical $\Sigma 3$ boundaries (twins) are particularly strong.
2. Other possible strong boundaries are not sufficiently numerous to be identified.
3. All other high boundaries have similarly low strength, independent of their Σ values.
4. In particular, low Σ, high angle boundaries, as a group, are not strong.
5. These results qualitatively agree with predictions based on the structural unit model.
6. This means that 1) Ni_3Al and Ir have similar boundary structure and 2) the fracture strength of an intergranularly brittle polycrystalline aggregate can be increased only by increasing the fraction of low angle and symmetrical $\Sigma 3$ boundaries.

References

1. T. Watanabe, *Materials Forum* **11**, 284 (1988).
2. L. C. Lim and T. Watanabe, *Acta metall.* **38**, 2507 (1990).
3. J. B. Brosse, R. Fillit and M. Biscondi, *Scripta metall.* **15**, 619 (1981).
4. A. Kobylanski and C. Goux, *C. R. Acad. Sci. Paris* **217**, 1937 (1971).
5. C. V. Kopetskii and A. I. Pashkovskii, *Sov. Phys. Dokl.* **18**, 340 (1973).
6. H. Kurishita, O. Akira, H. Kubo and H. Yoshinaga, *Trans. JIM* **26**, 341 (1985).
7. H. Kurishita, S. Kuba, H. Kubo and H. Yoshinaga, *Trans. JIM* **26**, 332 (1985).
8. S. Hanada, S. Watanabe and O. Izumi, *J. Mater. Sci.* **21**, 203 (1986).
9. S. S. Hecker, D. L. Rohr and D. F. Stein, *Metall. Trans.* **A 9A**, 481 (1978).
10. D. L. Rohr, L. E. Murr and S. S. Hecker, *Metall. Trans.* **10A**, 399 (1979).
11. C. T. Liu, H. Inouye and A. C. Schaffhauser, *Metall. Trans.* **A 12A**, 993 (1981).
12. T. Takasugi, E. P. George, D. P. Pope and O. Izumi, *Scripta metall.* **19**, 551 (1985).
13. C. T. Liu, C. L. White and J. A. Horton, *Acta metall.* **33**, 213 (1985).
14. P. H. Pumphrey, in *Grain boundary structure and properties* (Edited by G. A. Chadwick and D. A. Smith), Academic Press, London, 139 (1976).
15. V. Vitek, A. P. Sutton, D. A. Smith and R. C. Pond, in *Grain boundary structure and kinetics* (Edited by R. W. Balluffi), ASM, Metals Park, Ohio, 115 (1980).
16. P. J. Goodhew, in *Grain boundary structure and kinetics* (Edited by R. W. Balluffi), ASM, Metals Park, Ohio, 155 (1980).
17. N. L. Peterson, in *Grain boundary structure and kinetics* (Edited by R. W. Balluffi), ASM, Metals Park, Ohio, 209 (1980).
18. R. A. D. Mackenzie, M. D. Vaudin and S. S. L., in *Mat. Res. Soc. Symp. Proc.* **122**, 461 (1988).
19. D. Farkas, H. Jang, M. O. Lewus, R. Versaci and E. J. Savino, in *mat. Res. Soc. Symp. Proc.* **122**, 455 (1988).
20. T. Watanabe, *Res. Mechanica* **11**, 47 (1984).
21. L. C. Lim and R. Raj, *Acta metall.* **32**, 1183 (1983).
22. Measurements Group Inc, *Student Manual for Strain Gage Technology*, Bulletin 309B (1983).
23. H. Lin, PhD thesis, University of Pennsylvania, 62 (1991).
24. D. J. Dingley, *Scanning Electron Microscopy* **IV**, 273 (1981).
25. H. Mykura, in *Grain boundary structure and kinetics* (Edited by R. W. Balluffi), ASM, Metals Park, Ohio, 445 (1980).
26. Brandon, *Acta metall.* **14**, 1479 (1966).
27. H. Lin and D. P. Pope, *Acta Metallurgica Acta Metall.* in press (1992).
28. R. M. Bethea, B. S. Duran and T. L. Boullion, *Statistical Methods for Engineers and Scientists*, Marcel Dekker, New York and Basel, chapter 3 (1975).
29. D. H. Warrington, *J. Microscopy* **Pt 3**, 301 (1974).
30. A. P. Sutton and V. Vitek, *Phil. Trans. Roy. Soc.* **A309**, 1 (1983).
31. D. Schwartz, V. Vitek and A. P. Sutton, *Phil. Mag.* **A 51**, 499 (1985).
32. A. P. Sutton, *Phil. Mag.* **A 46**, 171 (1982).
33. A. P. Sutton, *Acta metall.* **36**, 1291 (1988).
34. M. Khantha, V. Vitek and M. Goldman, in *Proc. Mater. Res. Soc. Symp.* **193**, 349 (1990).
35. M. L. Jokl, V. Vitek, C. J. McMahon Jr and P. Burgers, *Acta metall.* **37**, 87 (1989).
36. W. T. Read and W. Shockley, *Phys. Rev.* **78**, 275 (1950).
37. V. Vitek, unpublished work (1989).
38. T. Takasugi and O. Izumi, *Acta metall.* **33**, 1247 (1985).
39. V. Vitek, S. P. Chen, A. F. Voter, J. J. Kruisman and J. T. M. DeHosson, *Materials Science Forum* **11**, 237 (1989).
40. R. P. Messmer and C. L. Briant, *Acta metall.* **30**, 457 (1982).
41. F. Chu, private communication (1992).
42. D. G. Pettifor, in *Ordered Intermetallics-Physical Metallurgy and Mechanical Behavior* (Edited by C. T. Liu, R. W. Cahn andG. Sauthoff), NATO Advanced Research Workshop, Irsee, Germany, (1991).